

Effect of Hydrogen on Hydrogen Permeation and Stress Corrosion Behavior of Low Alloy Steel in Acid Gas Field

Wang Xia, Zhou Wenjie, Hou Duo, Jiang Huan, Hou Li

College of Material Science and Engineering, Southwest Petroleum University, Chengdu 610500, China

Abstract: The effects of hydrogen concentration on hydrogen permeation and stress corrosion cracking behavior in 80SS low-alloy tubing steels in a saturated CO₂ simulated produced water environment were explored by electrochemical hydrogen permeation, slow strain rate tension and stereo microscope, SEM. The results show that the acidity and the hydrogen permeation parameters i^{∞} , D and C_0^H are both increased with the raise of the concentration of H⁺, which contributes to the diffusion behavior of hydrogen atoms. Since the synergistic effect of tensile stress and hydrogen atom, the fracture time of 80SS low alloy steel is reduced by nearly 50% compared with the tension in air, and the change occurs from ductile fracture to brittle fracture. As the hydrogen concentration of the solution increases, the mechanical damage of the steel and the stress corrosion sensitivity strengthen. Before and after pre-charged hydrogen the index I_s changes from 3.16% to 8.49% when 80SS steel is stretched in a medium containing saturated CO₂. Pre-charged hydrogen promotes the stress corrosion cracking sensitivity of the sample. When stretched in saturated CO₂ produced water containing 1wt% HAc, the microscopic morphology before pre-charged hydrogen shows a river pattern with quasi-cleavage fracture characteristics. Discontinuous cracks and small pores are distributed with fiber area of 80SS steel of the pre-charged hydrogen. Compared with before pre-charging, pre-charged hydrogen improves the plastic properties of the steel and reduces the stress corrosion cracking sensitivity of the steel.

Key words: 80SS low-alloy steel; hydrogen permeation; slow strain rate tension; pre-charged hydrogen; stress corrosion sensitivity; SEM

In recent years, with the continuous development of acidic oil fields and the wide use of CO₂ flooding technology, the mass fraction of acid gas such as H₂S/CO₂ in oil and gas resources rises, and low alloy steel faces the threat of corrosion of acid gas^[1-4]. Low-alloy oil casing steel is the lifeline for maintaining oil and gas wells, whose safety is of great significance to oil production. However, due to the complicated and harsh underground environment, a large number of tubing steels have corrosion cracking problems, resulting in heavy safety accidents and economic losses^[5-7]. CO₂ corrosion has also occurred in many oil fields in the United States, China and other countries, leading to serious results^[8-11]. In the oilfield production, it would interact with the metal material due to the infiltration and diffusion of hydrogen^[12], causing the material to become brittle and

cracked, loss of load carrying capacity^[13,14], and more likely to cause stress corrosion cracking, and steel fracture accidents^[15,16]. In the past, the research focused on the behavior of hydrogen permeation induced by the corrosion process of H₂S^[17-20], ignoring the effect of CO₂ environment on hydrogen permeation. But in fact, in the process of corrosion, CO₂ would not only cause corrosion of the material, but also cause hydrogen damage in the internal defects of the material^[21-23], and hydrogen damage was closely related to the diffusion behavior of hydrogen in the steel^[24]. Therefore, it is very important to explore the effect of hydrogen on the hydrogen permeation and stress corrosion behavior of low alloy tubing steel in CO₂ environment. In this study, the effects of hydrogen concentration on hydrogen permeation and stress corrosion cracking behavior in 80SS low-alloy

Received date: November 25, 2019

Foundation item: National Natural Science Foundation of China (51774242)

Corresponding author: Wang Xia, Professor, College of Materials Science and Engineering, Southwest Petroleum University, Chengdu 610500, P. R. China, E-mail: swpi_wx@126.com

Copyright © 2020, Northwest Institute for Nonferrous Metal Research. Published by Science Press. All rights reserved.

tubing steels in a saturated CO₂ simulated produced water environment were explored by electrochemical hydrogen permeation, slow strain rate stretching and stereo microscope, SEM. It provides a test basis for the effects of hydrogen permeability, stress corrosion cracking sensitivity and hydrogen permeation on stress corrosion behavior of low alloy steel in acid gas field environment.

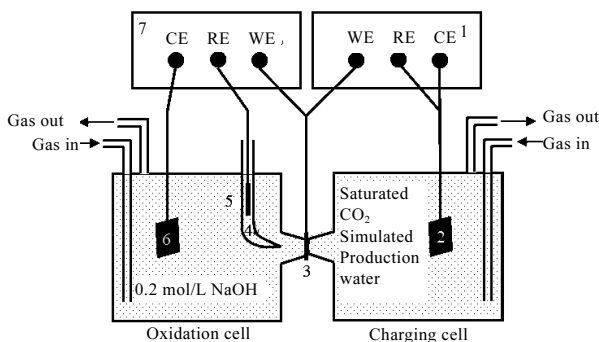
1 Experiment

The 80SS low alloy steel material was selected for the experiment, and its composition and content (wt%) were C 0.23, Si 0.27, Mn 0.54, P 0.012, S 0.005, Cr 1.01, Mo 0.32, Ni 0.03, V 0.006, Ti 0.007, Cu 0.02.

The experimental solution was simulated water containing saturated CO₂. According to the ionic composition (g/L) Na⁺ 12.89, K⁺ 12.18, Mg²⁺ 1.05, Ca²⁺ 0.88, Cl⁻ 32.92, SO₄²⁻ 3.23, HCO₃⁻ 0.6, Salinity 63.75, 2.5 L of simulated production water was prepared, and nitrogen gas was introduced for 4 h to remove oxygen and then introduced into CO₂ gas to saturation.

40 mm × 26 mm × 1 mm hydrogen permeable sheet sample was sanded to 1200# with water sandpaper, rinsed with deionized water, alcohol and acetone, and plated in Watt's nickel plating solution (250 g/L NiSO₄·6H₂O, 45 g/L NiCl₂·6H₂O, 40 g/L H₃BO₃) for 6 min at a current density of 1 mA/cm². A uniform nickel layer having a thickness of less than 0.2 μm was produced on the anode side.

Electrochemical testing of the Devanathan-Stachurski double electrolytic cell was carried out, which was assembled as shown in Fig.1. 0.2 mol/L NaOH solution was added to the anode chamber, and an anode polarization potential of 200 mV was applied. After the background current density was less than 0.2 μA/cm² and stabilized, saturated CO₂ simulated production water and different concentrations of HAc solution were added to the cathode chamber. The hydrogen permeation current versus time was tested.



1-ZF-9 Galvanometer, 2-Platinum electrode, 3-Sheet sample, 4-Salt bridge, 5-Saturated calomel electrode, 6-Platinum electrode, 7-CS 310 Electrochemical workstation

Fig.1 Hydrogen permeation experimental device

The slow strain rate tension samples were processed into sheets of the shape and size as shown in Fig.2.

The sample was sanded to 1200#, rinsed with deionized water, alcohol and acetone, and fixed in the experimental electrolytic cell. Except that the gauge length was exposed to the solution, the other part was coated with 704 silica gel in order to isolate the corrosion solution. Then the device was connected to the Stress Corrosion Cracking-1 Stress Corrosion Test System, injecting a corrosive medium solution (saturated CO₂ simulated production water + different concentrations of HAc solution), then a slow strain rate tensile test was performed, and the stretching rate was 5×10^{-5} mm/s.

The treated tensile specimens were pre-charged and immersed in saturated CO₂ simulated production water containing 1 wt% HAc for 48 h. The samples before and after pre-charging hydrogen were then subjected to slow strain rate tension test in saturated CO₂ simulated produced water and saturated CO₂ simulated produced water containing 1% HAc.

The slow strain rate tension test was carried out in 80SS steel in air and CO₂ simulated produced water with different HAc concentrations. The macroscopic morphology of the fracture was observed by XTL-500 stereo microscope.

The slow strain rate tension test was carried out on samples of 80SS steel in air and before and after pre-charging hydrogen in saturated CO₂ simulated produced water containing 1 wt% HAc. The morphology of the fracture was observed by EVO/MA15 scanning electron microscope (SEM).

2 Results and Discussion

2.1 Effect of solution hydrogen solubility on hydrogen permeation behavior

Fig.3 shows the hydrogen permeation curves of 80SS low alloy tubing steel at different HAc concentrations (C_{HAc}). The results show that the steady-state hydrogen permeation current density increases with the rise of HAc concentration. When the HAc was not added to the solution, the steady-state hydrogen permeation current of the 80SS steel improves from 0.3938 μA/cm² to 6.4543 μA/cm² as compared with the case where the HAc concentration is 2 wt%. This is mainly because in saturated CO₂ medium, the H⁺ content determines the hydrogen evolution reaction occurring in the cathode chamber. While the concentration of HAc increases, the pH of the solution decreases, the concentration of H⁺ in the solution, the rate of reaction and the number of generated hydrogen atoms increase, so the density of hydrogen

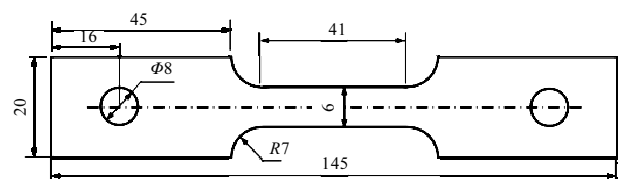


Fig.2 Slow strain rate tension sample shape and size

permeation increases^[25,26].

$$D = \frac{L^2}{8t_L} \quad (1)$$

$$C_0 = \frac{i^\infty L}{FD} \quad (2)$$

In the formula, L is sample thickness, mm; t_L is time corresponding to $i=0.432 i^\infty$, s; i^∞ is saturated anode current density, mA/cm²; F is Faraday constant, 96485 C/mol; D is effective diffusion coefficient of hydrogen, cm²/s.

The calculated hydrogen permeability coefficient D and the diffusible hydrogen concentration C_0^H data calculated by the Eq.(1) and (2) are shown in Table 1, and the corresponding trend is plotted in Fig.4. It is shown that the C_0^H rises as the HAc concentration escalates, because the pH value decreasing of the solution promotes hydrogen generation on the cathode side of the sample, so the diffusible hydrogen concentration increases. The overall trend of D hoisted with the rise of HAc concentration, but they do not show a linear relationship. This is mainly because D is usually related to the experimental conditions such as the material itself and temperature. When the pH value of the solution is smaller, the hydrogen concentration gradient on both sides of the sample is larger, and the diffusion power of the hydrogen atom is enhanced, thereby contributing more to the diffusion behavior of hydrogen^[27]; thus the hydrogen permeability coefficient is increased.

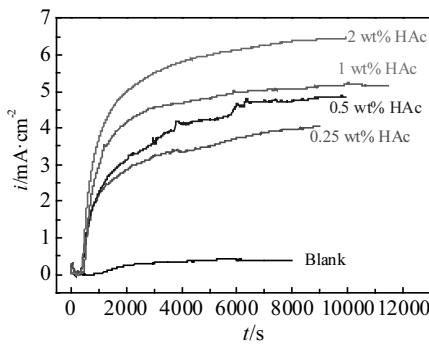


Fig.3 Hydrogen permeability curves at different HAc concentrations

Table 1 Fitted results of hydrogen permeation curves of 80ss low alloy tubing steel at different HAc concentrations

$C_{HAc}/wt\%$	$i^\infty/\mu A \cdot cm^{-2}$	$D/\times 10^{-6} cm^2 \cdot s^{-1}$	$C_0^H/mol H \cdot m^{-3}$
Blank	0.3938	0.769	0.53
0.25	4.0033	1.951	2.49
0.5	4.7324	1.981	3.07
1	5.1465	1.621	3.29
2	6.4543	1.922	3.99

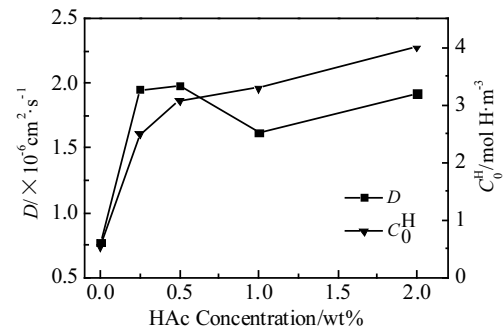


Fig.4 Relationship between D , C_0^H and HAc concentration

2.2 Effect of solution hydrogen solubility on slow strain rate tension

Fig.5 is a stress-strain curves of 80SS steel stretched in air and in different HAc concentrations solution. Table 2 shows the mechanical parameters. It can be found that the curves have no obvious yielding platform when HAc in the solution is not added. The stress decreases rapidly after the tensile strength, and the brittle fracture occurs after no significant necking stage. The fracture time is reduced by nearly 50%, and the steel exhibits poor plastic deformation, showing the brittle fracture characteristics.

The increase in acidity of the solution causes a significant decrease in yield strength and elongation after fracture, and the tensile strength is substantially unchanged. The addition of 2 wt% HAc concentration causes a bigger change in mechanical properties than when no HAc is added. The yield strength decreases from 515 MPa to 409 MPa, the elongation after fracture declines from 18.37% to 9.41%, which is reduced by nearly 50%. As the concentration of HAc increases, the higher the concentration of H^+ , the smaller the pH of the solution, and the mechanical damage caused by hydrogen to the steel is enhanced^[28].

The stress corrosion sensitivity is generally based on the elongation sensitivity index I_δ . When $I_\delta > 35\%$, the material has a significant stress corrosion tendency and is a hydro-

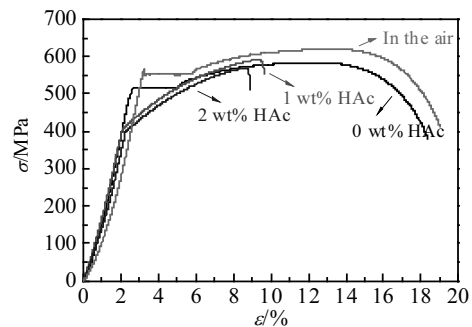


Fig.5 Stress-strain curves of 80SS stretching in air and in different HAc concentrations solution

gen embrittlement sensitive area. When $I_\delta < 25\%$, the material has no stress corrosion tendency and is a safe area. When I_δ is between 25% and 35%, it is a potential danger area^[29]. According to the calculation of formula(3), with the concentration of HAc in solution rising, the index I_δ increases correspondingly and exceeds 35%. The hydrogen embrittlement sensitivity of 80SS low alloy steel shows an increasing tendency and has a significant tendency of stress corrosion.

$$I_\delta = \frac{\delta_a - \delta_c}{\delta_a} \times 100\% \quad (3)$$

In the formula, δ_a is post-break elongation of the sample in air, %; δ_c is post-break elongation of the sample in a corrosive environment, %.

The macroscopic fracture morphology observed after the slow strain rate tension experiment in 80SS low alloy steel in air and in different HAc concentrations media is shown in Fig.6. The 80SS has a significant necking phenomenon in the fracture of the air. The material has excellent plasticity and exhibits ductile fracture characteristics. Due to the corrosive environment of acidic solution, when the HAc is not added, the fracture has a slight necking feature, but with the rising of HAc concentration, the area of the cross-sectional area of the section increases step by step, and the necking phenomenon gradually weakens and even disappears completely, showing a brittle fracture characteristic. This is because due to the hydrogen addition, the hydrogen in the solution adsorbs on the surface of the sample, diffuses into the crack tip, and accumulates at the stress concentration, thus reducing the bonding ability of the

atomic bond, making the region brittle and break with the action of tensile stress^[30].

2.3 Effect of hydrogen on stress corrosion behavior

Fig.7 is stress-strain curves of 80SS steel before and after pre-charging hydrogen in the two solutions, and Table 3 shows mechanical parameters. As seen from Fig.7a, when stretched in water medium containing saturated CO_2 , pre-charged hydrogen significantly reduces the yield strength and tensile strength, and decreases slightly the elongation. It shows that pre-charged hydrogen boosts the stress corrosion cracking sensitivity of the sample. It can be seen from Fig.7b that, in saturated CO_2 produced water containing 1wt% HAc, pre-charged hydrogen has little effect on the elastic phase and yield stage of the steel, but the tensile strength of the sample is lowered. The sample shows a necking stage and changes from brittle fracture to ductile fracture, indicating that pre-charged hydrogen increases the plastic properties of the steel and reduces the stress corrosion cracking sensitivity of the sample. As seen from Table 3, when 80SS steel is stretched in a medium containing saturated CO_2 , the index I_δ changes from 3.16% to 8.49%.

Table 2 Actual mechanical parameters of 80SS stretching in air and different HAc concentrations solution

$C_{\text{HAc}}/\text{wt}\%$	σ_c/MPa	σ_b/MPa	$\delta/\%$	$I_\delta/\%$
In the air	551	619	18.97	-
0	515	583	18.37	3.16
1	417	591	9.84	48.13
2	409	570	9.41	50.40

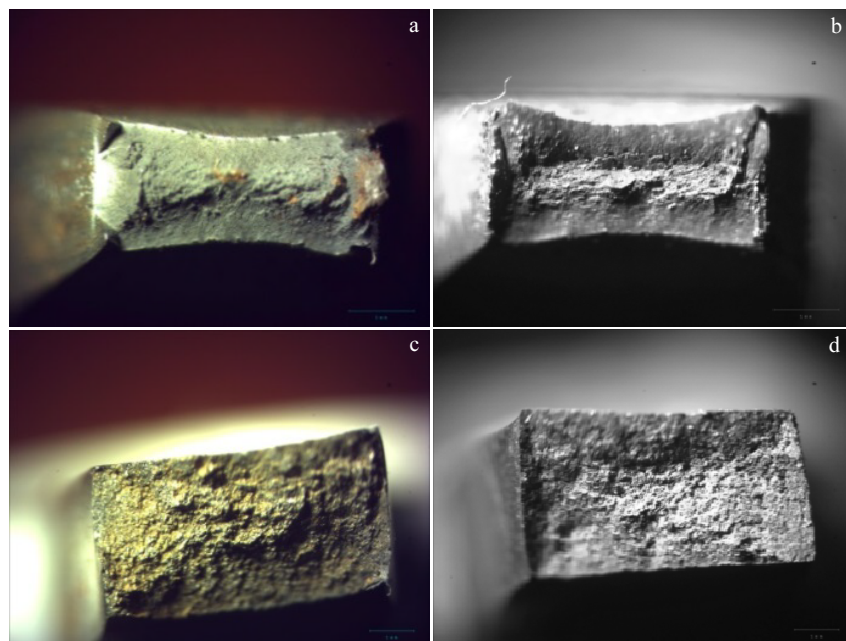


Fig.6 Fracture images of 80SS stretching in air (a) and in different HAc concentrations solution (b~d): (b) 0 wt%, (c) 1 wt%, and (d) 2 wt%

Pre-charged hydrogen in the two solutions has different effects on the sample. It is because during the pre-charging hydrogen process, a corrosion product film is formed on the surface of the metal surface due to the anodic reaction, and part of the atomic hydrogen generated by the cathodic reaction is adsorbed and enters the inside of the sample. When the slow strain rate tension test is stretched, the stress causes the metal to plastically deform, and the corrosion product film to rupture, which results in a local galvanic cell to form between the rupture film and the bare metal, and a local anodic dissolution reaction occurs. Therefore, the stress corrosion cracking sensitivity of 80SS steel in saturated CO_2 medium increases. However, in the saturated CO_2 produced water containing 1 wt% HAc, the H^+ concentration of the solution increases due to the addition of HAc, and the decrease in pH value promotes the formation of a new film covering after the product film is destroyed. Therefore, it has a certain hindrance to the entry of hydrogen atoms, reducing the stress corrosion cracking sensitivity^[31].

Fig.8 is SEM images of 80SS steel slow strain rate tension in air and before and after pre-charging hydrogen in saturated CO_2 produced water containing 1 wt% HAc. It can be seen from Fig.8a that the thickness of the fracture of 80SS steel changes from 3 mm to 1.15 mm when stretched in air and the necking phenomenon occurs. The fracture morphology is mainly uniform distribution of large and deep dimples. The sample exhibits ductile fracture characteristics, indicating that it has good plasticity in air.

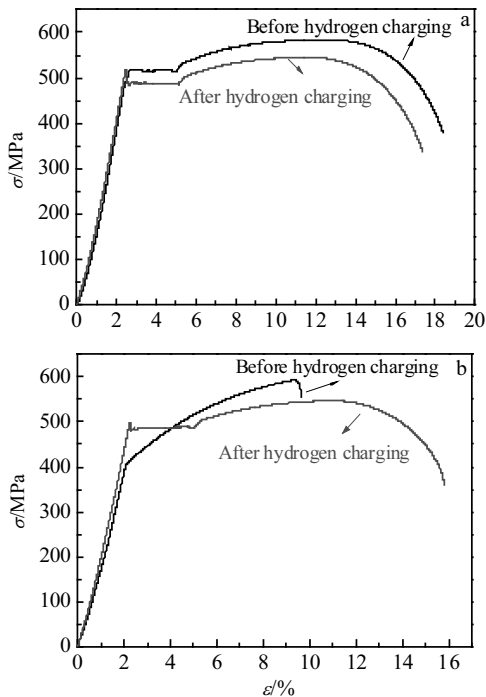


Fig.7 Stress-strain curves of 80SS steel before and after pre-charging hydrogen in two solutions: (a) saturated CO_2 produced water and (b) saturated CO_2 produced water containing 1 wt% HAc

Table 3 Actual measured mechanical parameters of 80SS steel before and after pre-charging hydrogen in two solutions

Stretching solution	Status	σ_e /MPa	σ_b /MPa	δ /%	I_δ /%
Produced water	Before	515	583	18.37	3.16
	After	486	544	17.36	8.49
Produced water +1% HAc	Before	417	591	9.84	48.13
	After	487	547	15.79	16.76

It can be seen from Fig.8b that compared with that in the air, the 80SS steel before pre-hydrogenation becomes flush and fractured in the acidic environment and is perpendicular to the tensile stress, and the microscopic appearance shows a river pattern. There are small cleavage planes and more tear ridges, and quasi-cleavage fracture characteristics occur. It shows that in the acidic environment, the hydrogen atoms enter the material since the dislocation of the material, so that the local plastic deformation of the material and the plasticity of the metal are reduced, and a certain degree of ductile-brittle transition occurs.

From Fig.8c, the tensile fracture after pre-charging hydrogen is slightly increased compared with that in air, and discontinuous cracks and small pore-like structures are distributed

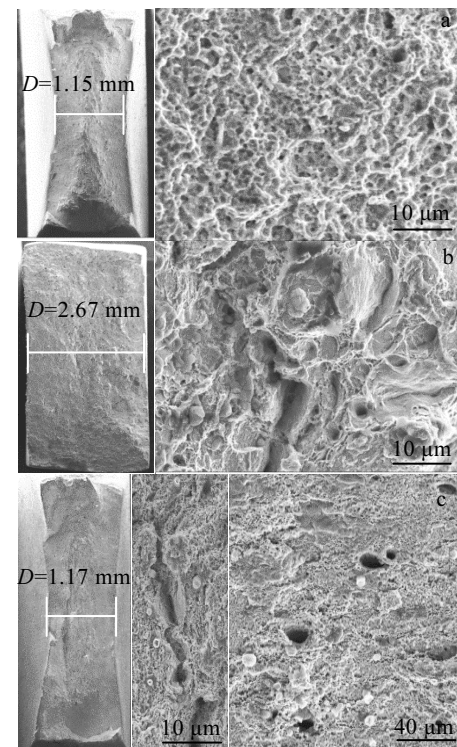


Fig.8 SEM images of fracture of 80SS steel in air and before and after pre-charging hydrogen in acid medium: (a) in the air (b) before pre-charging hydrogen in saturated CO_2 produced water containing 1 wt%HAc; (c) after pre-charging hydrogen+in saturated CO_2 produced water containing 1 wt% HAc

with the fiber region. This is mainly due to the distance of diffusion and diffusion of hydrogen inside the test piece gradually increases during the pre-charged hydrogen process. Due to the action of stress, the hydrogen pressure formed promotes the development of the micro-void and forms a larger crack. Compared with the tensile fracture before pre-charging hydrogen, the fracture after pre-charging hydrogen has a neck-shrinking phenomenon, showing better plasticity. Mainly because the material is sensitive to hydrogen, a small amount of hydrogen in the acidic solution will cause a change in the properties of the material, resulting in a decrease in the plasticity of the material. However, in the pre-charging hydrogen process, when the hydrogen content reaches a certain value, the degree of sensitivity increase becomes slower, and the degree of plasticity decrease becomes smaller^[32,33].

3 Conclusions

1) The acidity and the hydrogen permeation parameters i^∞ , D and C_0^H are both increased with the rise of the concentration of H^+ , which contribute to the diffusion behavior of hydrogen atoms.

2) The addition of HAc reduces the fracture time of 80SS low alloy steel by nearly 50%, reflecting the change from ductile fracture to brittle fracture. As the hydrogen concentration of the solution increases, the mechanical damage caused by the 80SS steel enhances, and the stress corrosion sensitivity of the steel strengthens.

3) When 80SS steel is stretched in a medium containing saturated CO_2 , the index I_δ changes from 3.16% to 8.49% after pre-charging hydrogen. Pre-charged hydrogen promoted the stress corrosion cracking sensitivity of the sample.

4) When stretched in saturated CO_2 produced water containing 1wt% HAc, the microscopic morphology of the tensile fracture before pre-charging hydrogen shows a river pattern with quasi-cleavage fracture characteristics. Discontinuous cracks and small pores are distributed with fiber area of 80SS steel of the pre-charged hydrogen. Compared with before pre-charging hydrogen, pre-charged hydrogen improves the plastic properties of the steel and reduces the stress corrosion cracking sensitivity of the steel.

References

- Ren C Q, Wang X, Liu L et al. *Materials and Corrosion*[J], 2012, 63(2): 168
- Zhang L, Ren B, Huang H D et al. *Journal of Petroleum Science and Engineering*[J], 2015, 125: 1
- Yuan C W, Zhang Z, Liu K J. *Fuel*[J], 2015, 142: 81
- Elgaddafi R, Naidu A, Ahmed R et al. *Journal of Natural Gas Science and Engineering*[J], 2015, 27(part_P3): 1620
- Liu Ranke, Zhang Deping, Hao Wenkui. *Journal of Sichuan University*[J], 2013(11): 196 (in Chinese)
- Ivan S C, Penny S S, Nick B. *International Journal of Greenhouse Gas Control*[J], 2011(5): 749
- Xie Tao, Lin Hai, Xu Jie et al. *Surface Technology*[J], 2017(1): 211 (in Chinese)
- Li Guomin, Li Aikui. *Journal of Materials Protection*[J], 2003, 36(6): 1 (in Chinese)
- Zhang Xueyuan, Yan Chao, Lei Liangcai. *Carbon Dioxide Corrosion and Control*[M]. Beijing: Chemical Industry Press, 2000: 2 (in Chinese)
- Li Helin, Lu Minxu. *New Progress in Corrosion Science and Anti-corrosion Engineering Technology*[M]. Beijing: Chemical Industry Press, 1999: 16 (in Chinese)
- Yaro A S, Abdul-Khalik K R, Khadom A A. *Journal of Loss Prevention in the Process Industries*[J], 2015, 38: 24
- Marie D, Stéphane P, Loïc M et al. *Corrosion Science*[J], 2014, 85: 251
- Sun Maocai. *Mechanical Properties of Metals*[M]. Harbin: Harbin Institute of Technology Press, 2003: 60 (in Chinese)
- Junichiro Y, Takuya M, Saburo M et al. *International Journal of Fracture*[J], 2012, 177(2): 141
- Deng Hongda, Li Chunfu, Cao Xianlong. *Petroleum and Natural Gas Chemical Industry*[J], 2011(3): 275 (in Chinese)
- Li Y F, Zhao L M, Kan W B et al. *International Journal of Hydrogen Energy*[J], 2012, 37(10): 8724
- Zhou C, Zheng S, Chen C et al. *Corrosion Science*[J], 2013, 67: 184
- Cheng Pan, Huang Feng, Zhao Xiaoyu et al. *Corrosion Science and Protection Technology*[J], 2016, 28(1): 21 (in Chinese)
- Plennevaux C, Kittel J, Frégonèse M et al. *Electrochemistry Communications*[J], 2013, 26: 17
- Huang F, Yuan W, Hu Q et al. *Advanced Materials Research*[J], 2013, 650: 72
- Tsayl W, Wu Yunfang, Wu J K et al. *Corrosion Science*[J], 2006, 48: 1926
- Zhi Zhang, Li C, Zhang J et al. *Journal of Wuhan University of Technology, Materials Science Edition*[J], 2012, 27(4): 657
- Hatami S, Ghaderi-Ardakani A, Niknejad-Khomami M et al. *The Journal of Supercritical Fluids*[J], 2016, 117: 108
- Briottet L, Moro I, Lemoine P. *International Journal of Hydrogen Energy*[J], 2012, 37(22): 17616
- Li Ping, Yan Yanqi, Hu Rumeng et al. *Corrosion Science and Protection Technology*[J], 2019, 31(4): 387 (in Chinese)
- Zhang T M, Zhao W M, Zhao Y J et al. *Int J Hydrogen Energy*[J], 2018, 43: 3353
- Wu H. *Thesis for Master*[D]. Nanchong: Southwest Petroleum University, 2014 (in Chinese)
- Lacoursiere M P, Aidun D K, Morrison D J. *Journal of Materials Engineering and Performance*[J], 2017, 26(5): 2337
- Zheng C B, Jiang H K, Huang Y L. *Corrosion Engineering Science and Technology*[J], 2011, 46(4): 365
- De Assis K S, Schuabb C G C, Lage M A et al. *Corrosion Science*[J], 2019, 152: 45

- 31 Tavares S S M, Bastos I N, Pardal J M et al. *International Journal of Hydrogen Energy*[J], 2015, 40(47): 16992
- 32 Sui F, Sandström R. *Materials Science and Engineering A*[J], 2016, 663: 108
- 33 Hu Haijun, Li Kang, Wu Wei et al. *Journal of Xi'an Jiaotong University*[J], 2016, 50(7): 89 (in Chinese)

氢对酸性气田低合金钢氢渗透及应力腐蚀行为的影响

王霞, 周雯洁, 侯铎, 蒋欢, 侯丽
(西南石油大学 材料科学与工程学院, 四川 成都 610500)

摘要: 采用电化学氢渗透、慢应变速率拉伸 (SSRT) 实验和体视显微镜、SEM 观察断口形貌的方法研究 80SS 低合金油管钢在饱和 CO₂ 模拟采出水环境中, 氢对氢渗透和应力腐蚀开裂行为的影响。结果表明, 随着溶液 H⁺ 浓度增大, 酸性的增加, 氢渗透参数 i^{∞} 、 D 和 C_0^H 均会增大, 有助于氢原子的扩散行为; 在拉应力和氢原子的协同作用下, 与空拉对比, 80SS 低合金钢的断裂时间减少了近 50%, 发生了由韧性断裂到脆性断裂的变化, 随着溶液氢浓度的增大, 对钢材引起的力学损伤增强, 应力腐蚀敏感性增大; 80SS 钢在含饱和 CO₂ 采出水介质中拉伸时, 预充氢前后的指数 I_b 由 3.16% 增大到 8.49%, 预充氢加大了试样的应力腐蚀开裂敏感性; 在含 1% HAc (质量分数) 的饱和 CO₂ 采出水中拉伸时, 预充氢前的微观形貌呈现出河流花样, 出现准解理断裂特征, 而预充氢后的 80SS 钢纤维区分布有不连续裂纹和小孔状结构, 与预充氢前的相比, 预充氢增加了钢的塑性性能, 降低了钢材的应力腐蚀开裂敏感性。

关键词: 80SS 低合金钢; 氢渗透; 慢应变拉伸; 预充氢; 应力腐蚀敏感性; SEM

作者简介: 王霞, 女, 1966 年生, 教授, 西南石油大学材料科学与工程学院, 四川 成都 610500, E-mail: swpi_wx@126.com